ASSESSMENT OF ELECTROMAGNETIC FIELD EMISSIONS FROM SUBSEA CABLES

Manhar Dhanak[1], R. Coulson, C. Dibiasio, J. Frankenfield, and E. Henderson
Florida Atlantic University,
Boca Raton, FL, USA

D. Pugsley and G. Valdes
Naval Surface Warfare Center,
Carderock Division,
Bethesda, MD, USA

[1]Corresponding author: Dhanak@fau.edu

INTRODUCTION

The characteristics of the electromagnetic (EM) field emissions from a subsea cable, based on subsurface field measurements and modeling, are described. The work is in support of characterizing the EM field emissions associated with subsea power transmission cables that will link marine hydrokinetic devices to shore, and assessment of their environmental impact on aquatic species. Previous studies suggest that several species can detect variability in the electric and magnetic fields in the water column and utilize them for navigation, searching for food and other life activities (see e.g. [1]). There is therefore some concern that anthropogenic sources of variability in the EM field may have negative impact on these species. The nature of EM field emissions from subsea cables depend on the transmitted power, whether the power supply is AC or DC, the frequency and amplitude of the AC current, cable construction, and whether the cable is monopole, bi-pole or tri-axial [2]. EM field emission levels from a power carrying cable decays inversely with distance from it. The electric field depends on the potential across the cable and increases with it while the magnetic field depends on the flow of current through the cable and increases with the magnitude of the current. A COWRIE report [3] concludes that, despite a number of modeling studies and laboratory and field experiments (see [4] for a review), the current state of knowledge regarding the EM field emitted by submerged power cables is variable and inconclusive and more field data on EM field emissions from subsea cables are needed in order to develop suitable predictive models. The overall aim of the present study was to develop a system for characterizing electric and magnetic field emissions from anthropogenic sources through field observations and physics-based modeling, in support of providing accurate predictive models of the emitted fields that are verified through comparison with field measurements.

MODELING EM FIELD EMISSIONS

The EM field emissions from a current carrying cable are modeled on the basis of Maxwell's equations for electromagnetic theory. The magnetic vector field $\vec{B}$ is estimated using the Biot-Savart law. For a cable carrying DC current, cable insulation typically prevents emission of the electric field. However, for one carrying AC current, an alternating magnetic field is generated [5], which in the conducting seawater induces an alternating electric field, $\vec{E}$, which is estimated using the Faradays' law of induction, $\nabla \times \vec{E} = -\frac{d\vec{B}}{dt}$. Theoretical modeling based EM fields emitted by a live straight cable are provided in [6].

AUV-BASED MEASUREMENT SYSTEM

Autonomous underwater vehicles (AUV) are suitable tether-free mobile sensor platforms for in-water surveys and have been demonstrated to provide good quality measurement of various physical variables (see for example, [7, 8]).

To measure and characterize the subsurface magnetic field, a SeaSPY magnetometer by Marine Magnetics Corporation is towed from a Bluefin 21 AUV through the water column by a 10m cable as schematically shown in Fig. 1 [9]. The SeaSPY is an Overhauser magnetometer that measures the total magnetic field with a sensitivity of 0.01nT and resolution of 0.001nT at a sampling rate of 1-4 Hz. The SeaSPY also includes a depth sensor and

operates at very low power levels, while maintaining its high sensitivity. The unit is powered via the tow cable by the AUV batteries. The sensors onboard the AUV include an upward (600kHz) and a downward (300kHz) looking ADCPs, a CTD package, a depth sensor and an Inertial Measurement Unit (IMU).

Electric field measurement in seawater is achieved through the use of two electrical points in contact with the seawater that are connected to a voltage-measuring device. The straight line between the two contacts gives the direction of the E-field. The measured voltage divided by the separation distance between the contact points gives the electric field, expressed in volts per meter. The contact points, or electrodes, are designed in such a way that they produce minimal voltage in the absence a source of electric field. The voltage measured by a two-electrode sensor depends on the electrode spacing. Three pairs of electrodes are orthogonally configured to provide a 3-axes E-field sensor. The sensing element is silver (Ag) which forms silver chloride (AgCl)) in seawater. It is non-polarizable and as such has relatively constant potential in response to small changes in current. Ag/AgCl sensors are robust and have excellent long-term stability [10,11].

The electrodes have a low contact resistance with the seawater, resulting in low noise levels [8]. Each is enclosed in a cup-like housing, filled with a saltwater agar bridge (Fig 2). Contact with the seawater is via this porous barrier, which minimizes contaminants from entering the chamber, shielding the electrode and helping to minimize biofouling. The housing also reduces the flow noise.

The six electrodes are located on the AUV hull as shown in Fig. 3 to provide 3-axes measurement of the E-field. To determine the local E-field, measured potentials across pairs of electrodes are amplified using a specially designed low-noise amplifier with a fixed gain of 1000 and then routed to a 3-channel simultaneously sampled A/D converter. The digitized data is stored for post-processing and a sub-sample of the data is also sent to the AUV for real-time monitoring. The electronics for data processing are located in a self-contained on-board pressure housing (Fig. 4). By combining the three axial components of the electric field, the total field vector can be computed regardless of the vehicle's orientation.

The sensors were extensively tested and calibrated in the laboratory for a range of fields produced by AC/DC sources through placing the sensors at known distances from the source and verifying the amplitude characteristics of the sensors. Laboratory tests will be described.

FIELD OBSERVATIONS

The site of the surveys was NSWC-CD's South Florida Ocean Measurement Facility (SFOMF, [12]) on the east coast of Florida, and the surveys were conducted over one of many live subsea cables seabed at the site. A number of EM field-measurement missions were conducted on the SFOMF range in the vicinity of the cable, with the power in the cable turned on/off. The AUV was required to perform 'lawnmower pattern surveys' at various altitudes above the cable, with legs 100-200m long and 40-50m apart as desired, at a speed of 1.5 m/s. Here we briefly describe illustrative results from two of the missions, one focused on measurement of the B-field using the towed magnetometer and the other focused on measuring the E-field. Subsequent development now allows simultaneous measurement of both the E and B-field. Fig. 5a shows an aerial view of the AUV and the towed magnetometer, while Fig 5b shows a view from a camera mounted onboard the towed magnetometer.

The AUV's lawn-mower pattern path across the cable, 4m above the bottom is shown in Fig. 6. The magentometer, towed 10m behind and 1.8m below the AUV, provides obsevations of the B-field at an altitude of 2.2m above the seafloor. The legs of the path are approximately 100m long and 40m apart. The survey was carried out with the power in the cable off and then repeated with the power turned on.

Fig. 7 shows the time series of the B-field measured as the AUV traversed across the cable as indicated in Fig. 6 for the cases of DC power in the cable on and off. The measurements include the background earth's magnetic field. As the sensor crosses the live cable, a peak in measurement of up to 150 μT is recorded. The characteristics of the signature as the cable is crossed depends on whether it is crossed from north to south or from south to north. This is because the measured total B-field includes the sum of the vertical component of the B-field emitted by the cable and that of the earth's magnetic field on one side of the cable, and a difference between the two on the other side. Fig. 8 shows the signature of the emitted B-field across the energized DC cable, obtained by subtracting the mean field across the cable. This is consistent with modeled B-fields [2].

The measurements shown in Fig. 7 are utilized together with the position information recorded by the AUV to develop a contour map of the B-field over the region as shown in Fig. 9 for the case of the energized DC cable; the position of the sensor lags that of the AUV by 11s as it is towed behind the vehicle through the water. The contour map is developed through interpolation of the B-field recorded by the sensor as it is towed

along the lawn-mower pattern path (shown superimposed in the figure). The mean B-field value at this altitude is appproximately 30 nT above ambient, that is, when the power in the cable is turned off.

A second pair of surveys illustrated here involve one conducted along the same path as shown in Fig. 6, but this time to determine the E-field emitted by the submerged cable carrying a 10 Hz AC current in comparison with the background field (with the power in the cable turned off). Fig. 10 shows the time-series of the root-mean-square of the measured E-field at an altitude of 4m above the seafloor in the cases with the power in the cable turned on and with it turned off. The background field has a mean value less than $10\mu V/\text{m}$. In comparison, the E-field emissions when the power is turned on reach values of up to over $60\mu V/\text{m}$, the values peaking as the cable is crossed. Fig. 11 shows the signature of the emitted E-field across the energized AC cable, obtained by subtracting the mean field across the cable.

As in the case of the B-field, the measurements shown in Fig. 10 are utilized together with the position information recorded by the AUV to develop a contour map of the E-field over the region as shown in Fig. 12 for the case with the power in the cable turned on. Since the ambient E-field is small, the field over the surveyed region is dominated by the emissions from the cable. The mean E-field value at this altitude is $22\mu V/m$ above ambient. The dashed lines mark the ± 2.5 x standard deviation of the ambient field. The white line tentatively indicates the location of the cable (as estimated by Lat-Long coordinates available at the time the cable was laid). The observations suggest that the cable has shifted from its original location, likely through the action of sediment transportation.

DISCUSSION

EM field sensors, including a SeaSPY magnetometer and a custom E-field sensor, have been implemented on a Bluefin 21 AUV. The SeaSPY is towed 10m behind the vehicle while the 3-axes Ag/AgCl E-field sensor is located on the AUV. The measured data are processed, digitized and stored on board the AUV together with data from other sensors. The buoyancy and trim of the vehicle as well as the electric ground arrangement on the standard SeaSPY had to be modified as part of the implementation. The sensor tows well and analysis of the results suggest that good quality measurements can be made using the arrangement discussed here. Recent modifications allow simultaneous measurement of the E and B-fields during a single mission. The magnetic field computed using Biot-Savart Law, corresponding to case depicted in Fig. 6 is shown in Fig. 13. Comparison of the modeled field may be made with field observations in Fig. 9. The observations will serve as a database, in support of validating predictive models of the EM emissions from submerged cables. Further analysis of acquired data is underway.

Fig. 1: Schematics of towing the SeaSPY magnetometer using an AUV

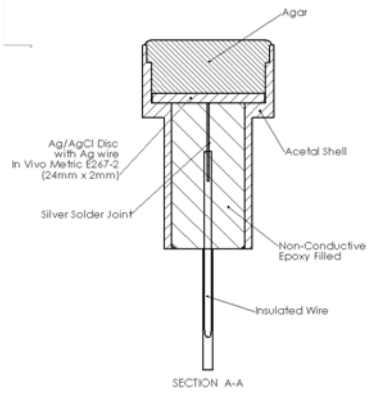

Fig. 2: Ag/AgCl Electrode

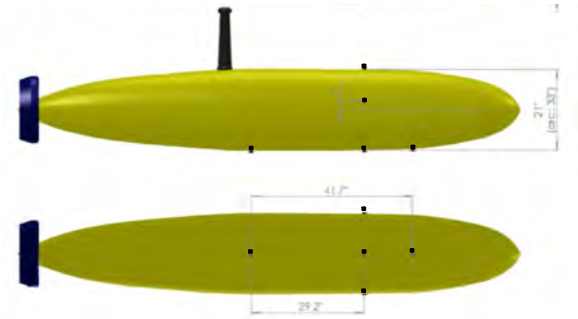

Fig.3: Location of the electrodes (black appendages) on the AUV hull. Side and bottom views are shown in order.

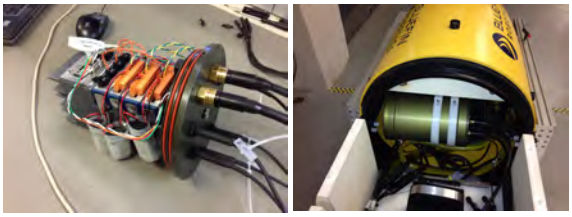

Fig.4: E-Field processing unit and pressure vessel onboard the AUV

Fig. 5: AUV-towed magnetometer. (a) Aerial view, (b) View from the towed sensor

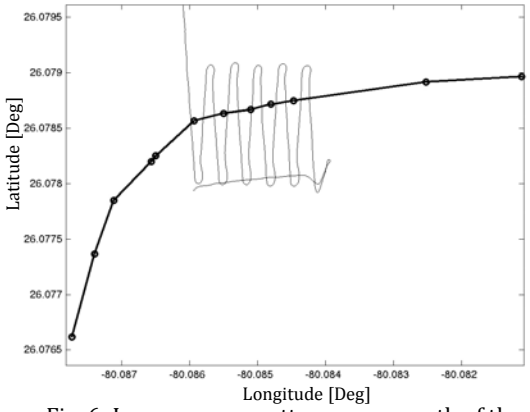

Fig. 6: Lawn-mower pattern survey path of the AUV at a depth of 4m across the expected location of the cable (thick black line)

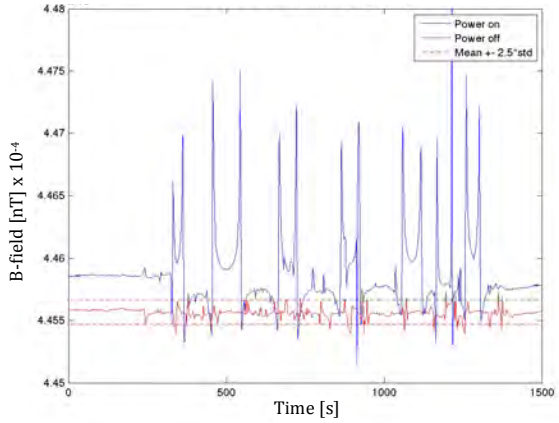

Fig. 7: B-field measured as the AUV traverses the path over the cable indicated in Fig. 6, for the DC power in the cable on and off. The dashed lines mark the ± 2.5 x standard deviation of the ambient field

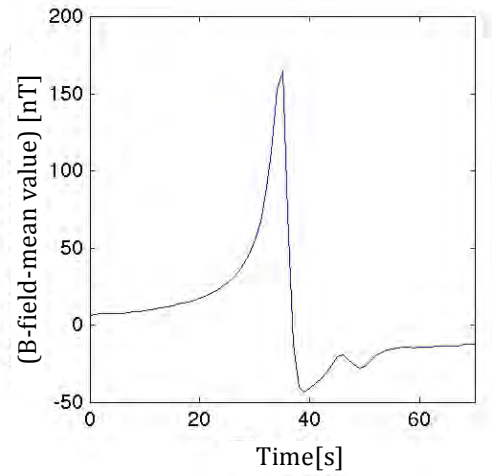

Fig. 8: Measured B-field signature during crossing of an energized DC cable

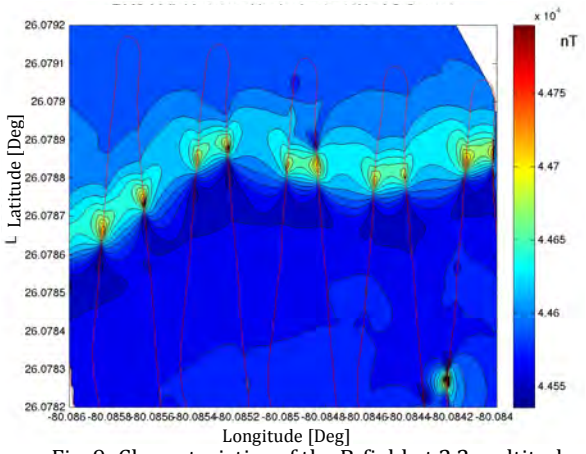

Fig. 9: Characteristics of the B-field at 2.2m altitude above a submarine cable energized with DC power. The lawn-mower pattern path of the AUV is superimposed on the contour map.

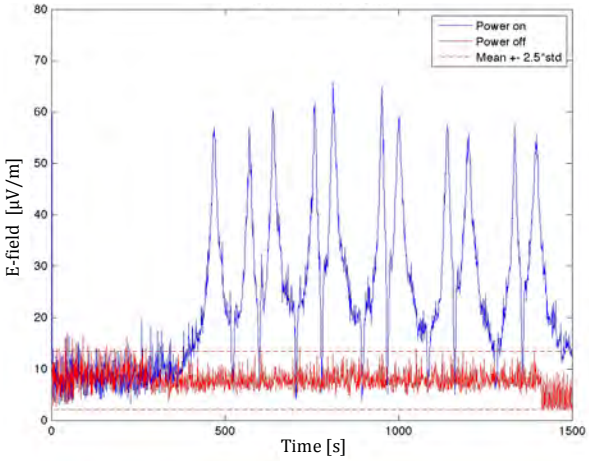

Fig. 10: RMS of the measured E-field as the AUV traversed at 4m altitude over the cable as indicated in Fig. 6 for the cases with 10Hz AC current in the cable turned on and off

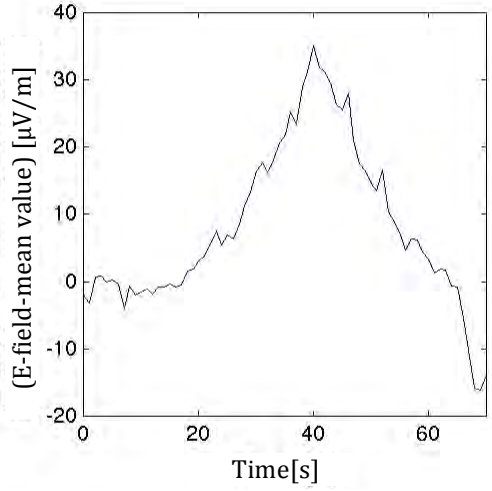

Fig. 11: RMS E-field signature during crossing of an energized 10Hz AC cable by the AUV

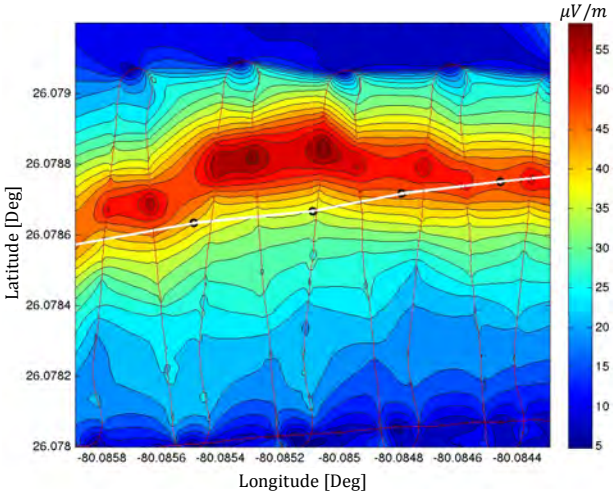

Fig. 12: E-field 4m above a subsea cable energized with 10Hz AC power.

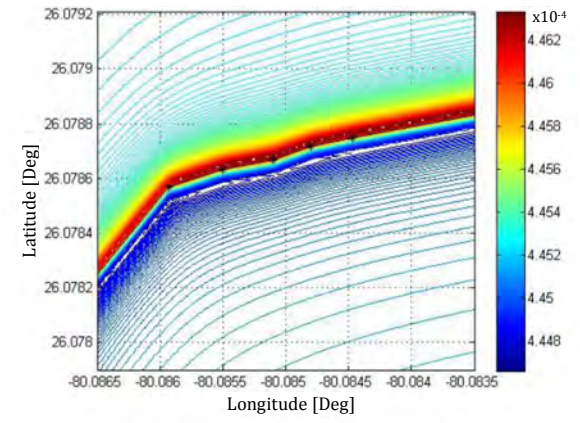

Fig. 13: Modeled magnetic field distribution corresponding to case depicted in Fig. 9.

ACKNOWLEDGEMENT

The work is supported by the US Department of Energy (Award: DE-EE0006386).

REFERENCES

[1] Gill, A.B., I Gloyne-Philips, J Kimber, P Sigray, 2014. "Marine Renewable Energy, Electromagnetic (EM) Fields and EM-Sensitive Animals" Marine Renewable Energy Technology and Environmental Interactions Editors: Mark A. Shields, Andrew I.L. Payne. Springer. Chapter 6, pp 61 -80.

[2] M. Slater, R. Jones, and A. Schultz, "Electromagnetic field study" Oregon Wave Energy Trust, 2010.

[3] COWRIE Report. "A Baseline Assessment of Electromagnetic Fields Generated by Offshore Windfarm Cables," University of Liverpool, UK. 2003.

[4] Tricas, Timothy and Andrew Gill 'Effects of EMFs from Undersea Power Cables on Elasmobranchs and Other Marine Species.' 2011. Final Report. U.S. Department of the Interior. Bureau of Ocean Energy Management, Regulation, and Enforcement.

[5] Dhanak, M. R., An, E, Holappa, K., 2001. An AUV survey in the littoral zone: small-scale subsurface variability accompanying synoptic observations of surface currents. IEEE J. Oceanic Eng. Vol 26 (4)

[6] Olsson, Thomas, Peter Bergsten, Johan Nissen, and Anette Larsson. 2010. Impact of EMF from Sub-sea cables on marine organisms. Final Report. Vattenfall Ocean Energy Programme. Stockholm, Sweden.

[7] E. An, M. R. Dhanak, L. K. Shay, S. Smith and J. Van Leer. Coastal oceanography using an AUV. J. Atmos. & Ocean Tech., vol 18 (2), pp215-234.

[8] Dhanak, Manhar, E. An, R. Coulson, J Frankenfield, W. Venezia, K von Ellenrieder. 2013. 'Magnetic Field Surveys of Coastal Waters Using an AUV-Towed Magnetometer.' MTS/IEEE Oceans Conference, San Diego, CA USA

[9] Havsgård, Geir Bjarte. 'Low noise Ag/AgCl electric field sensor system for marine CSEM and MT applications', 2011. Marelec Conference, La Jolla, SanDiego, CA, USA. June, 2011.

[10] Zhendong Wang, Ming Deng*, Kai Chen, and Meng Wang. An Ultralow-Noise Ag/AgCl Electric Field Sensor with Good Stability for Marine EM Applications. 2013 Proceedings of the Seventh International Conference on Sensing Technology. 751-754.

[11] W. Venezia et al., "SFOMC, A Successful Navy And Academic Partnership Providing Sustained Ocean Observation Capabilities in the Florida Straits," MTS Journal, Vol. 37, 81-91, 2003.